Vol. 42 (2011) ACTA PHYSICA POLONICA B No 7

THE DRELL–YAN PROCESSES AT FORWARD RAPIDITIES AT THE LHC*

Emilia Lewandowska

The Henryk Niewodniczański Institute of Nuclear Physics
Polish Academy of Sciences
Radzikowskiego 152, Kraków, Poland
emilia.lewandowska@ifj.edu.pl

(Received May 6, 2011)

The analysis of the Drell–Yan lepton pair production at forward rapidities at the Large Hadron Collider is presented, using the dipole approach with saturation effects.

DOI:10.5506/APhysPolB.42.1497
PACS numbers: 12.38.Bx, 13.60.Hb

1. Introduction

The Large Hadron Collider (LHC) opens a new kinematic regime at high energies. In this regime, QCD evolution leads to fast growth of a gluon density. At high density novel phenomena related to saturation of the gluon density due to non-linear QCD evolution equations will occur [1]. The Drell–Yan processes at forward rapidities at the LHC offer a new way to study these affects in the hadronic scattering environment [2].

2. Drell–Yan cross-section in the collinear approach

The Drell–Yan production is a unique process which offers high sensitivity to the parton distribution functions in hadrons. In the leading order (LO) approximation, the Drell–Yan lepton pair of invariant mass ($M > 1$ GeV) is produced by annihilation of two quarks from the colliding hadrons, see the diagram in Fig. 1,

$$q_f\bar{q}_f \to \gamma^* \to l^+l^- \,.$$

* Presented at the Cracow Epiphany Conference on the First Year of the LHC, Cracow, Poland, January 10–12, 2011.

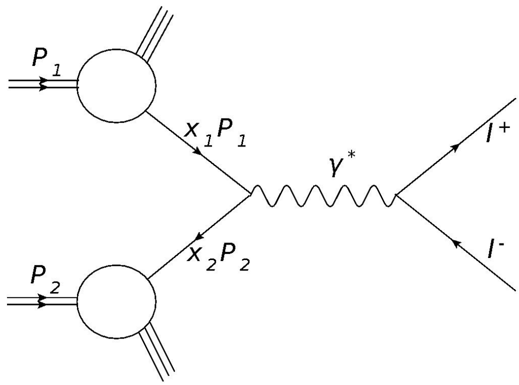

Fig. 1. The Drell–Yan lepton pair production.

The cross-section in this approximation is given by the quark/antiquark distributions in the colliding hadrons taken at the scale M^2

$$\frac{d^2\sigma^{\mathrm{LO}}}{dM^2 dx_{\mathrm{F}}} = \frac{4\pi\alpha_{\mathrm{em}}^2}{3N_c M^4}\frac{x_1x_2}{x_1+x_2}\sum_f e_f^2 \times \left\{q_f\left(x_1,M^2\right)\bar{q}_f\left(x_2,M^2\right)+\bar{q}_f\left(x_1,M^2\right)q_f\left(x_2,M^2\right)\right\}, \quad (1)$$

where α_{em} is the fine structure coupling constant, N_c is the number of quark colors and $q_f, \bar{q}_f$ are quark/antiquark distributions. The quark momentum fractions, x_1 and x_2, are determined by the lepton pair kinematics

$$x_1 = \frac{1}{2}\left(\sqrt{x_{\mathrm{F}}^2+4\frac{M^2}{s}}+x_{\mathrm{F}}\right), \qquad x_2 = \frac{1}{2}\left(\sqrt{x_{\mathrm{F}}^2+4\frac{M^2}{s}}-x_{\mathrm{F}}\right), \quad (2)$$

where $x_{\mathrm{F}} = x_1 - x_2$ is the Feynman variable of the lepton pair and s is the hadronic center-of-mass energy squared.

In the next-to-leading (NLO) approximation additional emissions of a parton into the final state has to be taken into account, see the diagrams in Fig. 2. Because of the emission, one of the quarks entering the photon vertex carries a fraction $z < 1$ of the incoming parton momentum. Thus, the incoming parton momentum fractions take now the form

$$x_1 = \frac{1}{2}\left(\sqrt{x_{\mathrm{F}}^2+4\frac{M^2}{zs}}+x_{\mathrm{F}}\right), \qquad x_2 = \frac{1}{2}\left(\sqrt{x_{\mathrm{F}}^2+4\frac{M^2}{zs}}-x_{\mathrm{F}}\right). \quad (3)$$

The NLO corrections to the Drell–Yan cross-section are proportional to the strong coupling constant α_{s} and are given by [3, 4, 5]

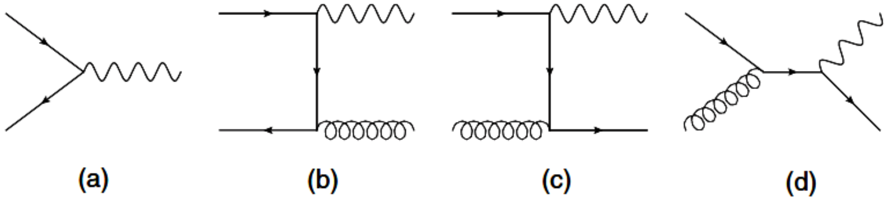

Fig. 2. The Drell–Yan production in the leading (a) and next-no-leading (b)–(d) order approximation. The diagrams (c) and (d) are enhanced in the small-x limit due to a strongly rising gluon distribution.

$$\begin{aligned}\frac{d^2\sigma^{\mathrm{NLO}}}{dM^2dx_{\mathrm{F}}} &= \frac{4\pi\alpha_{\mathrm{em}}^2}{3N_cM^4}\frac{\alpha_{\mathrm{s}}(M^2)}{2\pi}\int\limits_{z_{\min}}^{1} dz\frac{x_1x_2}{x_1+x_2} \\ &\times\sum_f e_f^2\Big\{q_f\left(x_1,M^2\right)\bar{q}_f\left(x_2,M^2\right)D_q(z)+g\left(x_1,M^2\right) \\ &\times\left[q_f\left(x_1,M^2\right)+\bar{q}_f\left(x_2,M^2\right)\right]D_g(z)+(x_1\leftrightarrow x_2)\Big\}\,, \end{aligned} \tag{4}$$

where the coefficient functions $D_{q,g}$ are calculated perturbatively and g is a gluon distribution. Thus, up to the order α_{s}, the Drell–Yan cross-section in the collinear approach is the sum of the leading and next-to-leading contributions

$$\frac{d^2\sigma^{\mathrm{col}}}{dM^2dx_{\mathrm{F}}} = \frac{d^2\sigma^{\mathrm{LO}}}{dM^2dx_{\mathrm{F}}} + \frac{d^2\sigma^{\mathrm{NLO}}}{dM^2dx_{\mathrm{F}}}\,. \tag{5}$$

3. Drell–Yan process in the small-x limit

In the small-x limit, the dilepton mass is much smaller than the center-of-mass energy of the colliding hadrons, $M \ll \sqrt{s}$. In this case, a momentum fraction of one of the incoming partons is very small, *e.g.*

$$x_1 \sim 1\,, \qquad x_2 = \frac{M^2}{s\,x_1} \ll 1\,. \tag{6}$$

If the small momentum fraction is carried by a gluon, the fast incoming quark probes high gluon density system in which saturation effects may occur.

The target rest frame point of view is particularly attractive for physical interpretation of these effects. In this frame, the fast incoming quark interacts with the target gluon field before or after scattering, emitting a virtual photon. This is shown by diagrams in Fig. 3. The photon then decays producing a lepton pair which moves into the region of forward rapidity.

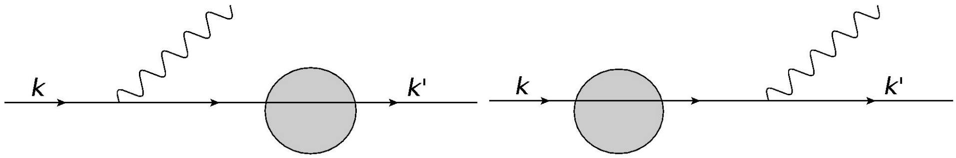

Fig. 3. The Drell–Yan process in the target rest frame point of view.

The cross-section for radiation of a photon with the momentum fraction z of the fast quark is given by [6]

$$\sigma(qp \to \gamma^* X) = \int d^2r \, W\left(z, r, M^2\right) \sigma_{qq}(x_2, zr) \,, \tag{7}$$

where r is the photon–quark transverse separation and W is the photon wave function squared, computed perturbatively in [7,8]. The dipole cross-section σ_{qq} [9] is known from DIS scattering at small Bjorken-x and describes the interaction of the incoming quark with strong gluon fields of the target hadron. The dipole form comes from the interference of the two shown amplitudes in the formula for the cross-section. The final form of the Drell–Yan cross-section in the dipole framework is given by the equation

$$\frac{d^2\sigma^{\mathrm{DY}}}{dM^2 \, dx_{\mathrm{F}}} = \frac{\alpha_{\mathrm{em}}}{6\pi M^2} \frac{1}{x_1 + x_2} \int_{x_1}^{1} \frac{dz}{z} F_2\left(\frac{x_1}{z}, M^2\right) \sigma(qp \to \gamma^* X) \,, \tag{8}$$

where F_2 is the proton structure function. We will compare predictions given by this formula with those given by the collinear factorization approach (5). Before presenting our results, we will describe the dipole cross-sections used in the analysis.

3.1. Dipole cross-section models

The following three models of the dipole cross-sections σ_{qq} with gluon saturation effects have been used in the calculations:

- Golec-Biernat–Wüsthoff (GBW) [10,11]

$$\sigma_{qq}(x, r) = \sigma_0 \left\{1 - \exp\left(-r^2 Q_{\mathrm{s}}^2(x)/4\right)\right\} \,, \tag{9}$$

- Bartels–Golec–Kowalski–Sapeta (BGKS) [12, 13]

$$\sigma_{qq}(x,r) = \sigma_0 \left\{1 - \exp\left(-\pi^2 r^2 \alpha_{\mathrm{s}}\left(\mu^2\right) xg\left(x,\mu^2\right)/3\sigma_0\right)\right\}\,, \tag{10}$$

- Color Glass Condensate (CGC) [14, 15]

$$\sigma_{qq}(x,r) = \sigma_0 \times \begin{cases} N_0 \left(\frac{rQ_{\mathrm{s}}}{2}\right)^{2\left(\gamma_{\mathrm{s}}+\frac{1}{\kappa\lambda Y}\ln\frac{2}{rQ_{\mathrm{s}}}\right)} & : \quad rQ_{\mathrm{s}} \leq 2\,, \\ 1 - e^{-A\ln^2(B\,rQ_{\mathrm{s}})} & : \quad rQ_{\mathrm{s}} > 2\,. \end{cases} \tag{11}$$

In the formulas, Q_{s} is the saturation scale: $Q_{\mathrm{s}} = Q_0\,x^{-\lambda}$. The parameters in the above formulas are determined from the analysis of the HERA data on deep inelastic scattering.

4. Results

In Fig. 4 we present a comparison of the results from the collinear factorization (5) and the dipole approach (8) formulas with the existing data from the Fermilab E772 Collaboration [16]. We use the NLO CTEQ6.6M parton

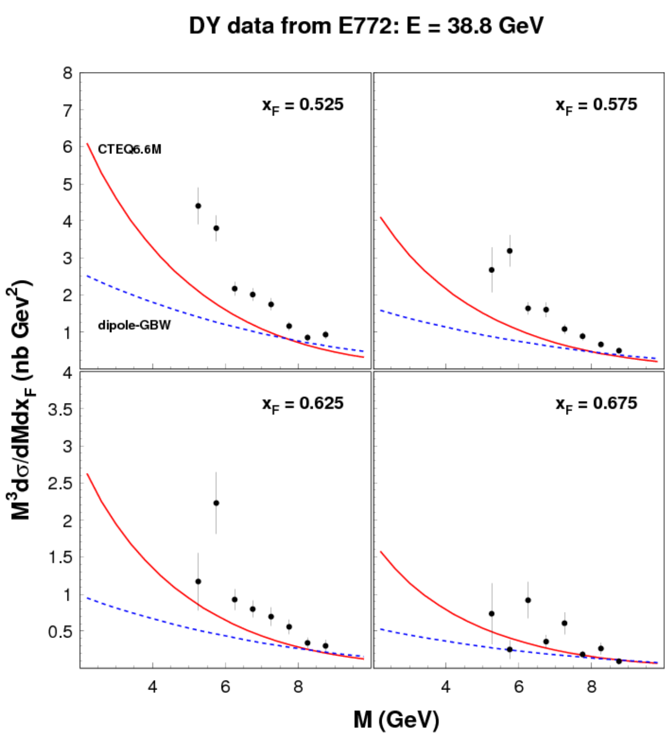

Fig. 4. The Drell–Yan cross-section from the collinear and dipole approaches against the E772 Collaboration data.

distributions [17] for the collinear factorization and the GBW parametrization [10,11] for the dipole cross-section. It is clearly seen that for the different values of the Feynman variable x_{F}, the E772 data are above the results from both approaches.

Fig. 5 presents predictions for the Drell–Yan cross-section as a function of the center-of-mass energy $\sqrt{s}$ at fixed $x_{\mathrm{F}} = 0.15$ for three values of the lepton pair mass $M = 6, 8, 10$ GeV. At the LHC energy, saturation effects in the dipole model give results which are significantly below the collinear factorization predictions. The same results are shown using the linear scale in Fig. 6. The CTEQ6.6M and MSTW08 parton distributions, and the GBW and BGKS [12, 13] dipole models are used in these plots. The CGC model (11) gives results which are very close to the GBW lines.

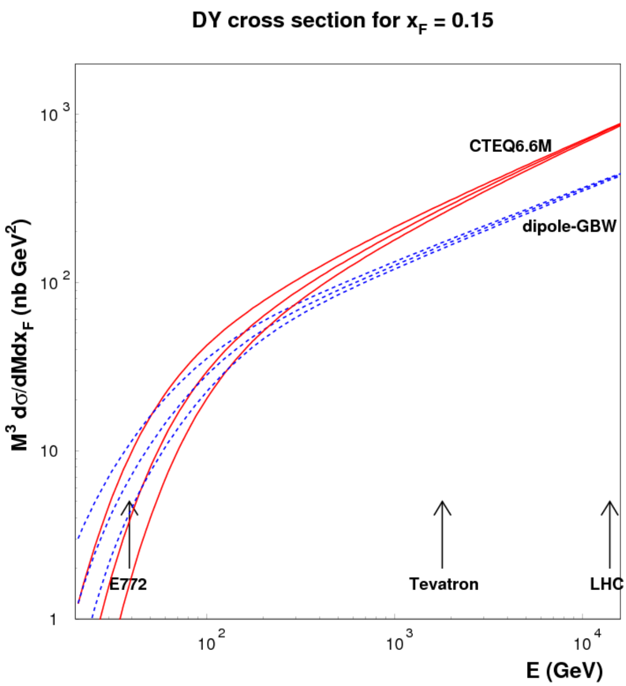

Fig. 5. The DY cross-section from the collinear and dipole approaches as a function of energy $E = \sqrt{s}$ for fixed $x_{\mathrm{F}} = 0.15$ and lepton pair mass $M = 6, 8, 10$ GeV.

Thus, the predictions from the dipole approach with gluon saturation give a significant suppression of the Drell–Yan production cross-section in comparison to the collinear factorization results. We are looking forward to the experimental verification of this result.

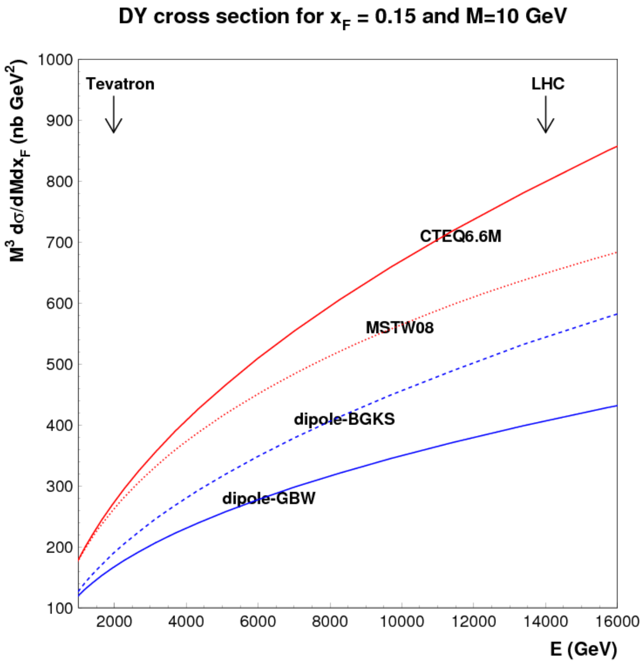

Fig. 6. The DY cross-section from the collinear and dipole approaches for fixed $x_{\mathrm{F}} = 0.15$ and dilepton mass $M = 10$ GeV.

5. Summary

We presented the analysis of the Drell–Yan lepton pair production at forward rapidities at the LHC. We compare two predictions, from the standard collinear factorization approach and from the dipole approach with gluon saturation effects. The latter prediction gives significantly lower value for the total cross-section than the standard one without saturation effects.

REFERENCES

[1] L.V. Gribov, E.M. Levin, M.G. Ryskin, *Phys. Rep.* **100**, 1 (1983).

[2] K. Golec-Biernat, E. Lewandowska, A.M. Staśto, *Phys. Rev.* **D82**, 094010 (2010).

[3] G. Altarelli, R.K. Ellis, G. Martinelli, *Nucl. Phys.* **B143**, 521 (1978).

[4] G. Altarelli, R.K. Ellis, G. Martinelli, *Nucl. Phys.* **B157**, 461 (1979).

[5] J. Kubar-Andre, F.E. Paige, *Phys. Rev.* **D19**, 221 (1979).

[6] B.Z. Kopeliovich, J. Raufeisen, A.V. Tarasov, *Phys. Lett.* **B503**, 91 (2001).

[7] S.J. Brodsky, A. Hebecker, E. Quack, *Phys. Rev.* **D55**, 2584 (1997).

[8] M.A. Betemps, M.B. Gay Ducati, M.V.T. Machado, *Phys. Rev.* **D66**, 014018 (2002).

[9] N.N. Nikolaev, B.G. Zakharov, *Z. Phys.* **C49**, 607 (1991).

[10] K. Golec-Biernat, M. Wusthoff, *Phys. Rev.* **D59**, 014017 (1999).

[11] K. Golec-Biernat, M. Wusthoff, *Phys. Rev.* **D60**, 114023 (1999).

[12] J. Bartels, K. Golec-Biernat, H. Kowalski, *Phys. Rev.* **D66**, 014001 (2002).

[13] K.J. Golec-Biernat, S. Sapeta *Phys. Rev* **D74**, 054032 (2006).

[14] E. Iancu, K. Itakura, S. Munier, *Phys. Lett.* **B590**, 199 (2004).

[15] G. Soyez, *Phys. Lett.* **B655**, 32 (2007).

[16] P.L. McGaughey *et al.*, *Phys. Rev.* **D50**, 3038 (1994).

[17] P.M. Nadolsky *et al.*, *Phys. Rev.* **D78**, 013004 (2008).